

Intensity-dependent effects in the Beam Delivery System of ILC 250 GeV and 500 GeV

P. Korysko
University of Oxford
CERN



Outline

- Introduction
- Impact of short-range wakefields on the vertical beam size at the IP in both 250 GeV and 500 GeV ILC BDS.
- Impact of long-range wakefields on the vertical beam deflection at the IP and the luminosity in both 250 GeV and 500 GeV ILC BDS.
- Conclusions

Acknowledgements

Special thanks to:

- Philip Burrows from the University of Oxford.
- Andrea Latina and Daniel Schulte from CERN.
- Angeles Faus-Golfe from IJCLab.

Introduction

The International Linear Collider

The International Linear Collider (ILC) is a 250–500 GeV (extendable to 1 TeV) centre-of-mass high-luminosity linear electron-positron collider, based on 1.3 GHz superconducting radio-frequency accelerating technology. ILC parameters and technologies are summarized in the ILC Technical Design Report (2013) [1].

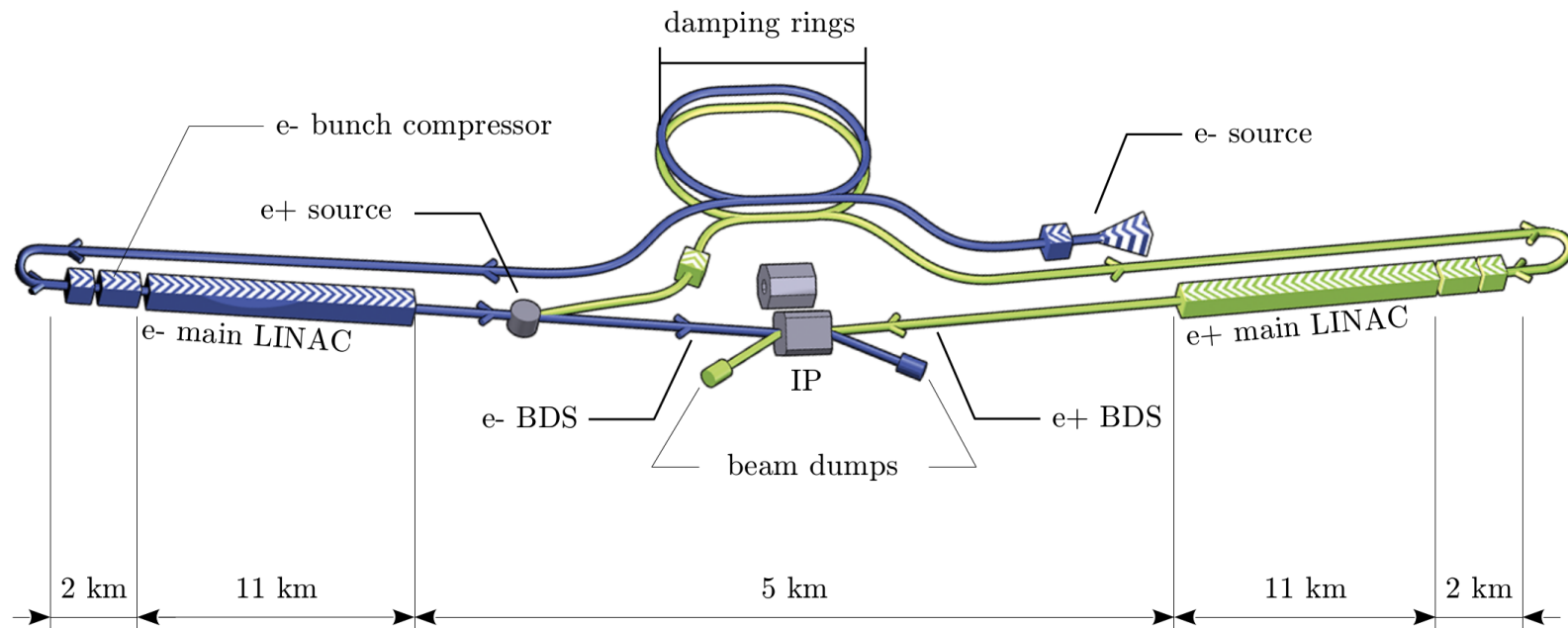


Figure: ILC 500 GeV layout with dimensions (not to scale)

Introduction

The ILC Beam Delivery System (BDS)

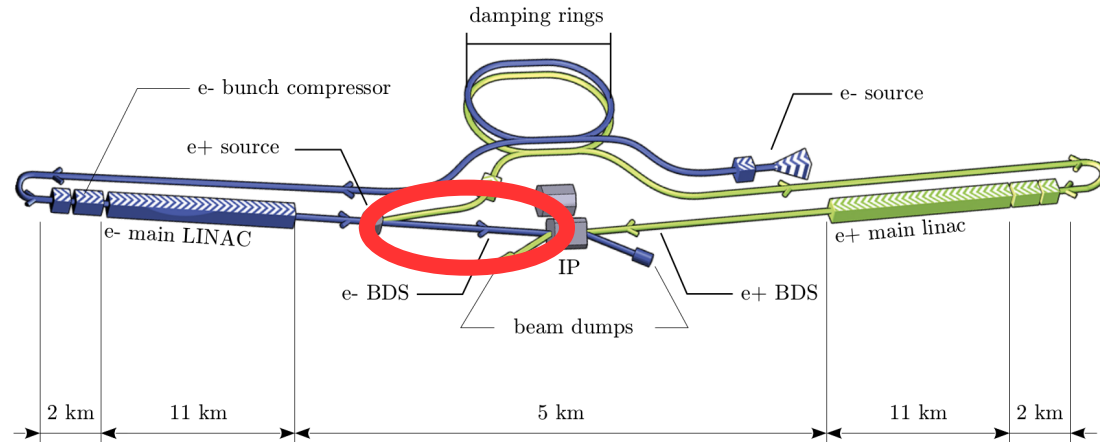


Table: ILC 250 GeV beam parameters.

| Parameter | Symbol | Value |
|-----------------------|-------------------------|--------------------------|
| Centre-of-mass energy | E_{CM} | 250 GeV |
| Length of the BDS | L_{BDS} | 2254 m |
| Number of bunches | n_b | 1312 |
| Bunch population | N | $2.0 \times 10^{10} e^-$ |
| RMS bunch length | σ_z | 0.3 mm |
| Bunch separation | Δt_b | 554 ns |
| IP RMS beam sizes | σ_x^*/σ_y^* | 516/7.7 nm |

Table: 500 GeV ILC beam parameters.

| Parameter | Symbol | Value |
|-----------------------|-------------------------|--------------------------|
| Centre-of-mass energy | E_{CM} | 500 GeV |
| Length of the BDS | L_{BDS} | 2254 m |
| Number of bunches | n_b | 1312 |
| Bunch population | N | $2.0 \times 10^{10} e^-$ |
| RMS bunch length | σ_z | 0.3 mm |
| Bunch separation | Δt_b | 554 ns |
| IP RMS beam sizes | σ_x^*/σ_y^* | 474/5.9 nm |

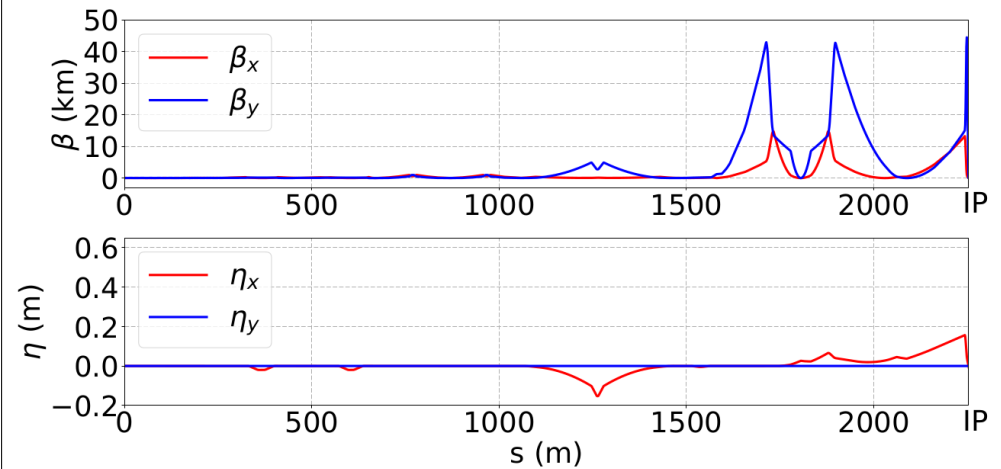


Figure: The ILC BDS 500 GeV Twiss parameters calculated with PLACET

Introduction

The ILC Beam Delivery System (BDS)

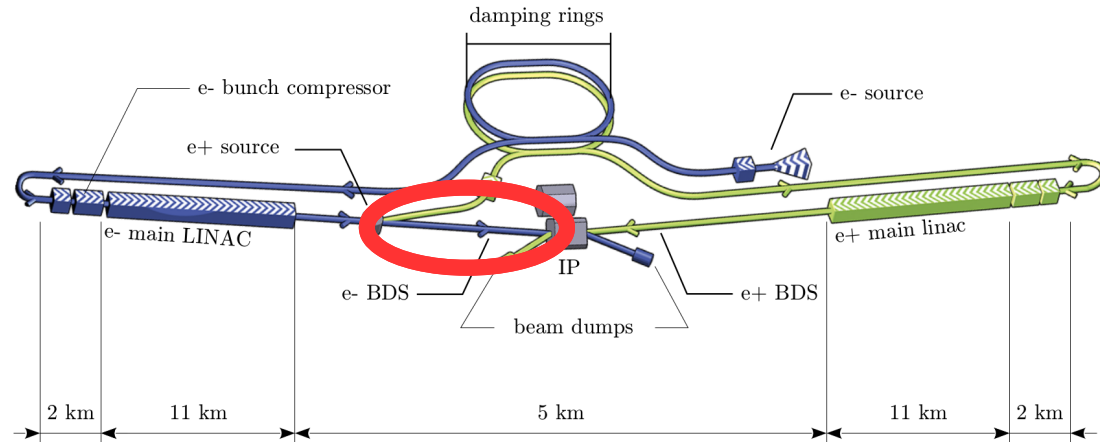


Table: ILC 250 GeV beam parameters.

| Parameter | Symbol | Value |
|-----------------------|-------------------------|--------------------------|
| Centre-of-mass energy | E_{CM} | 250 GeV |
| Length of the BDS | L_{BDS} | 2254 m |
| Number of bunches | n_b | 1312 |
| Bunch population | N | $2.0 \times 10^{10} e^-$ |
| RMS bunch length | σ_z | 0.3 mm |
| Bunch separation | Δt_b | 884 ns |
| IP RMS beam sizes | σ_x^*/σ_y^* | 516/7.7 nm |

Table: 500 GeV ILC beam parameters.

| Parameter | Symbol | Value |
|-----------------------|-------------------------|--------------------------|
| Centre-of-mass energy | E_{CM} | 500 GeV |
| Length of the BDS | L_{BDS} | 2254 m |
| Number of bunches | n_b | 1312 |
| Bunch population | N | $2.0 \times 10^{10} e^-$ |
| RMS bunch length | σ_z | 0.3 mm |
| Bunch separation | Δt_b | 884 ns |
| IP RMS beam sizes | σ_x^*/σ_y^* | 474/5.9 nm |

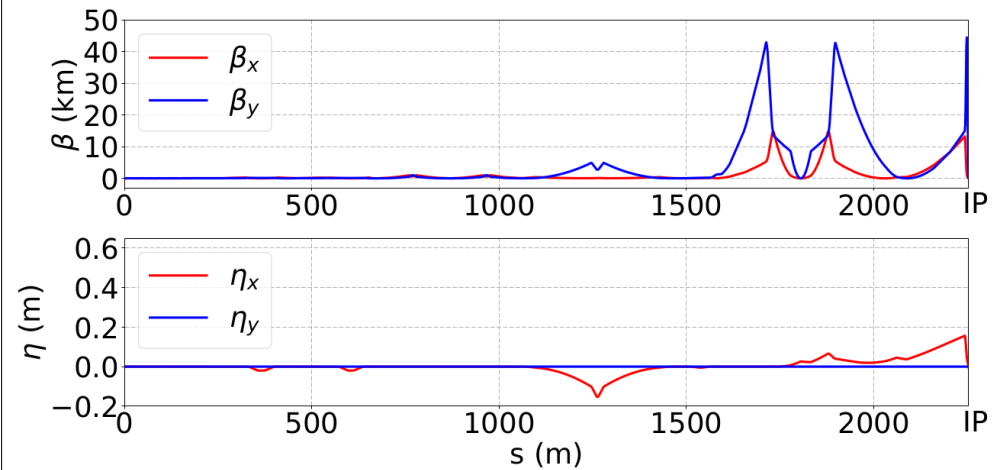


Figure: The ILC BDS 500 GeV Twiss parameters calculated with PLACET

Introduction

Transverse and longitudinal wakefields

The integrated fields seen by a test particle traveling on the same, or on a parallel path at a constant distance s behind a point charge Q are called the integrated longitudinal and transverse wakepotentials. They are defined as:

$$\tilde{W}_{\perp}(\Delta r, s) = \frac{1}{Q} \int_0^L [E_{\perp}(\Delta r, z, s) + c\hat{z} \times B(\Delta r, z, s)] dz$$

$$\tilde{W}_{\parallel}(s) = -\frac{1}{Q} \int_0^L [E_z(z, s)] dz$$

The transverse and longitudinal kicks felt by a particle, at position z along the bunch, due to all leading particles ($\forall z' : z' > z$):

$$\Delta r' = \frac{\Delta P_{\perp}}{P} = \frac{qQL}{Pc} \int_{-\infty}^z W_{\perp}(\Delta r(z'), z - z') \rho(z') dz'$$

$$\Delta P_{\parallel} = \frac{qQL}{c} \int_{-\infty}^z W_{\parallel}(z - z') \rho(z') dz'$$

with:

- $\rho(z')$ normalized line charge density of the bunch, such that $\int_{-\infty}^{\infty} \rho(z') dz' = 1$
- $\Delta r(z')$ transverse radial position of the leading particles as a function of their position z' along the bunch [mm]
- Q total charge of the bunch [C]

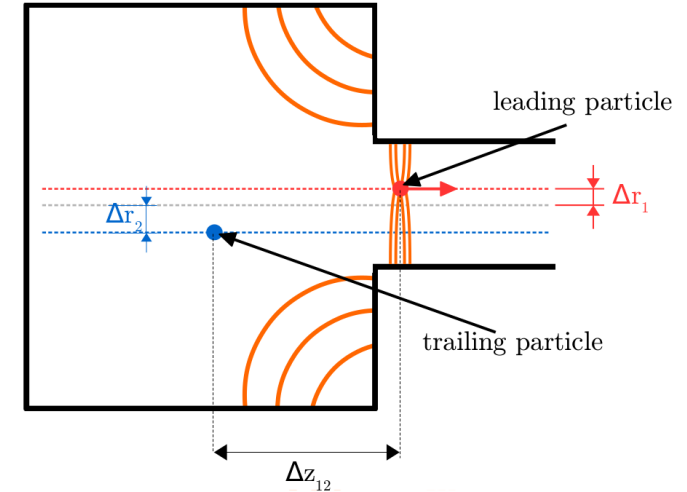


Figure: Scheme of the two-particle model.

- q particle's charge [e]
- P particle's momentum [eV/c]
- $\Delta r'$ radial kick [rad]
- ΔP momentum loss [eV]

Simulations of the impact of short-range wakefields in the ILC

Impact of corrections and intensity dependent effects

ILC orbit correction (1/3)

One-to-one correction

The One-to-one correction consists of minimizing the transverse position of the beam, with respect to the beam pipe centre measured at BPMs, using steering magnets [2].

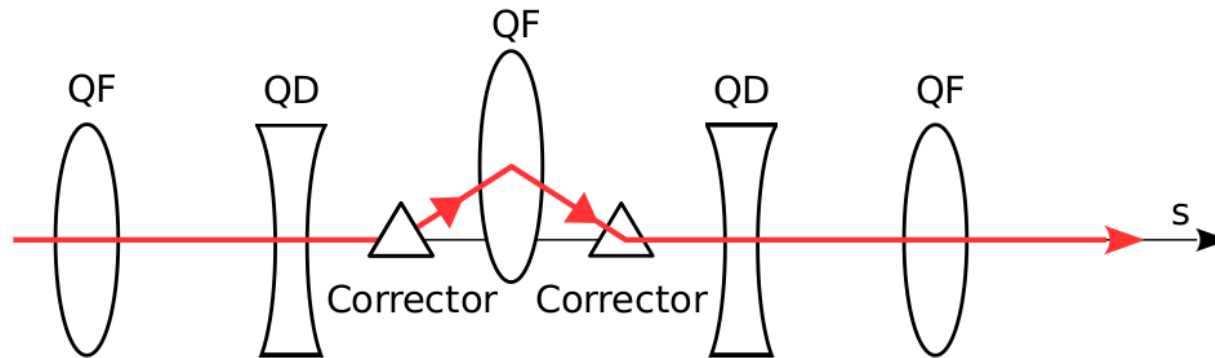


Figure: Schematic of the One-to-one correction. The beam orbit (in red) is deflected by correctors (triangles) in order to pass through the center of the BPM, which is inside a quadrupole in this case.

ILC orbit correction (2/3)

Dispersion Free Steering (DFS) correction

In the simulations, two beams are tracked with two different energies, E_1 and E_2 . Steering magnets are then used to correct the orbit and reduce the orbit difference between the two beams $\Delta_{y,E}$ [3].

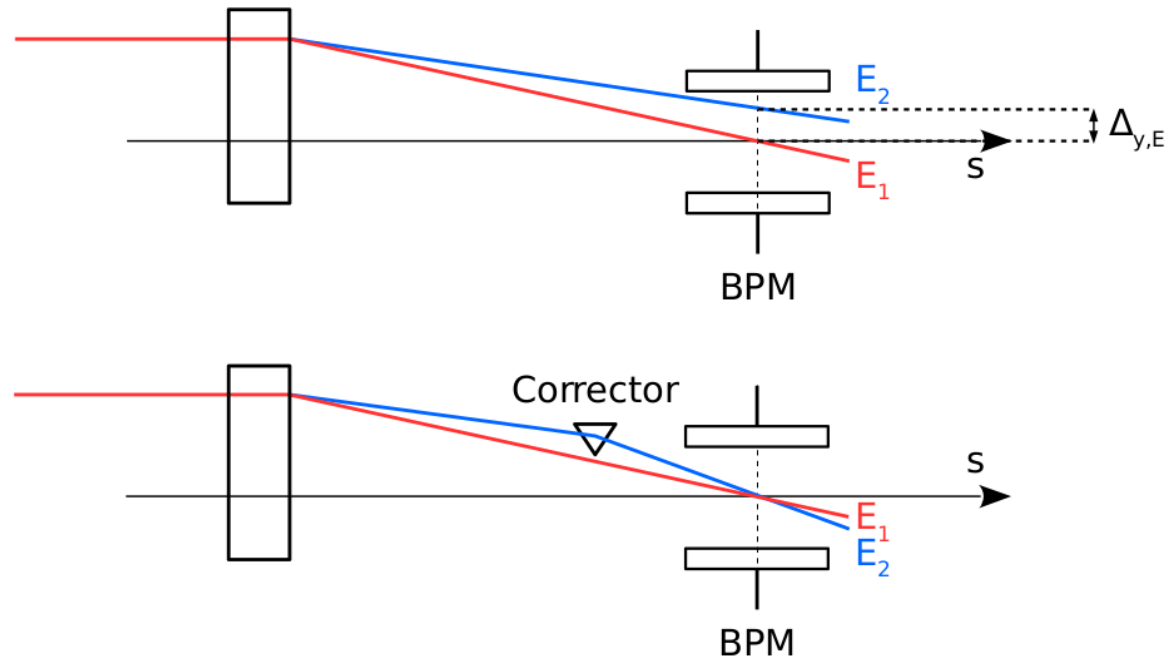


Figure: Schematic of the Dispersion Free Steering correction.

ILC orbit correction (3/3)

Dispersion Free Steering (DFS) correction

The Wakefield Free Steering is an algorithm which corrects the difference on the orbit introduced by wakefields. In the simulations, two beams are tracked with two different charges Q_1 and Q_2 . Steering magnets are then used to correct the orbit and reduce the orbit difference between the two beams $\Delta_{y,Q}$ [4].

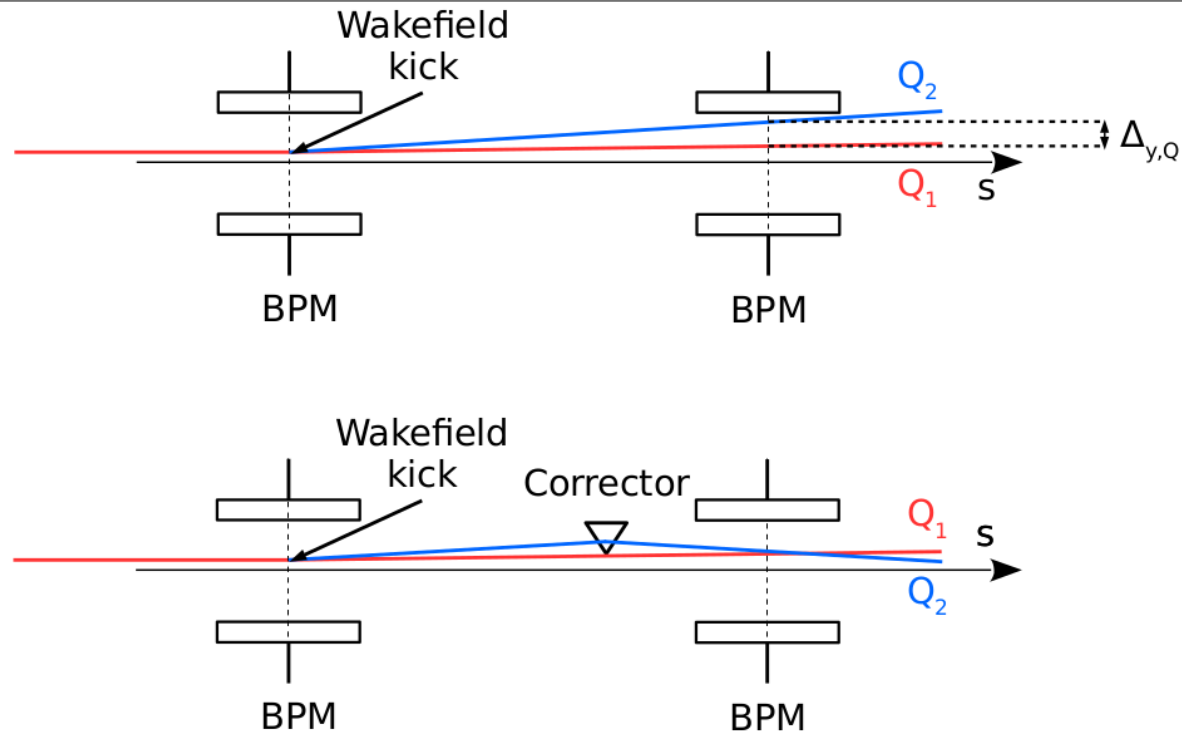


Figure: Schematic of the Wakefields Free Steering corrections.

Sextupole knobs

- First order knobs correction by changing the position of final focus sextupoles.
- Second order knobs correction by changing the strength of the final focus sextupoles.

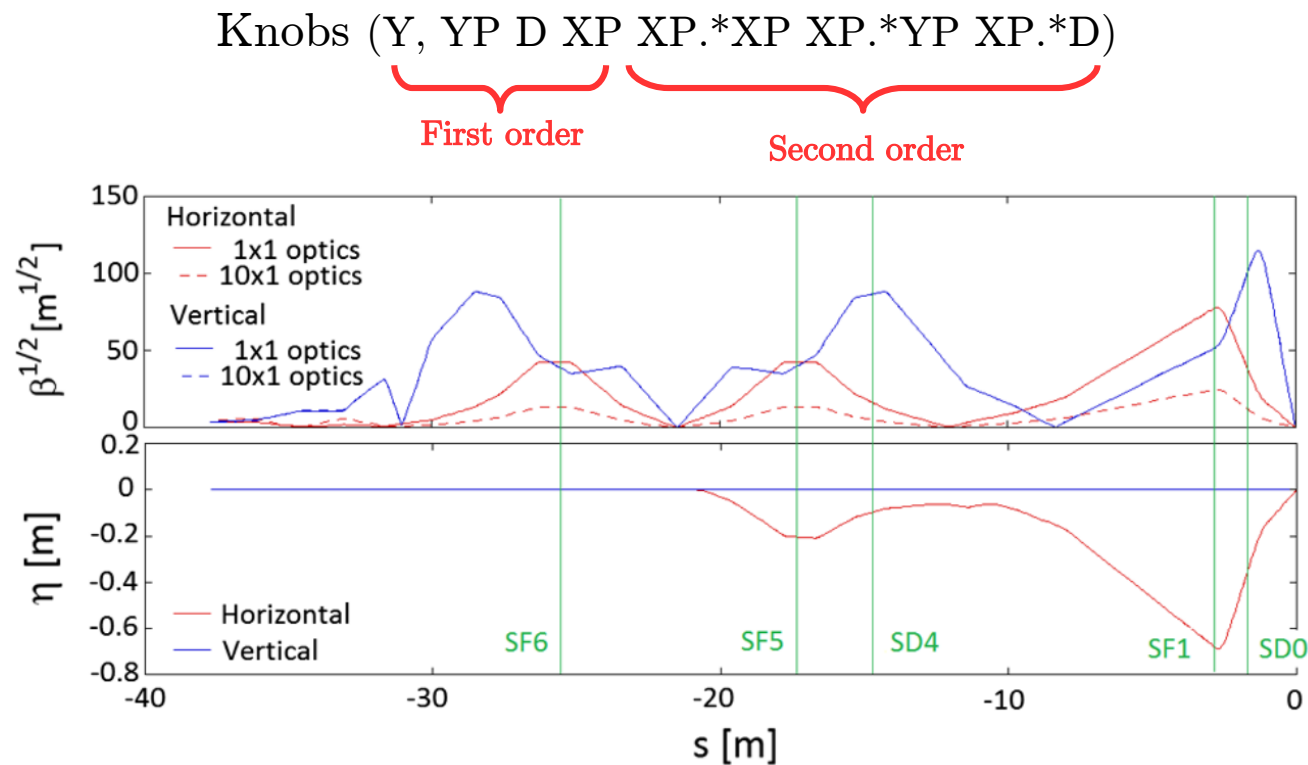


Figure: Positions of the sextupole knobs in the Accelerator Test Facility 2 (ATF2) [5].

Impact of corrections in ILC

Simulation conditions (1/2)

Simulated errors:

- Static errors:
 - Misalignment of quadrupoles, sextupoles and BPMs of $50\ \mu\text{m}$ RMS.
 - Strength error of quadrupoles and sextupoles of 0.1%.
 - Roll error for quadrupoles and sextupoles of $200\ \mu\text{rad}$.

Corrections applied:

- One-to-one
- DFS
- WFS
- Knobs (Y, YP D XP XP.*XP XP.*YP XP.*D)

First order Second order

Simulation procedure:

- 100 machines with the previously cited static imperfections.
- Apply the cited corrections and the knobs on the distribution at the IP.
- Measure the vertical beam size at the IP.

Impact of corrections in ILC Simulation conditions (2/2)

Wakefield sources: C-band cavity BPMs (C-BPMs), wakepotentials calculated with GdfidL [6][7][8].

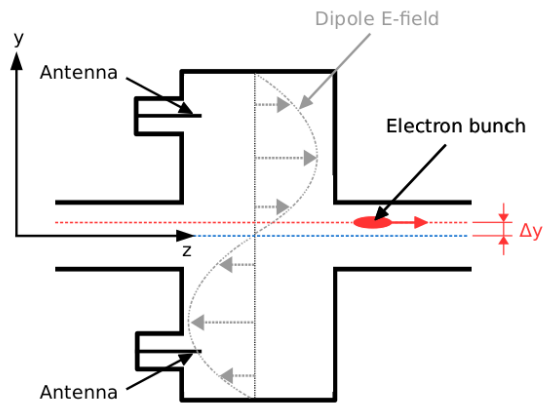
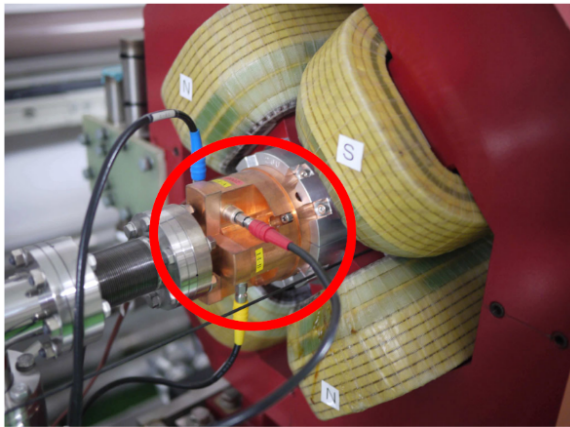


Figure: Picture of an ATF2 C-BPM (top) and schematic of a C-BPM (bottom).

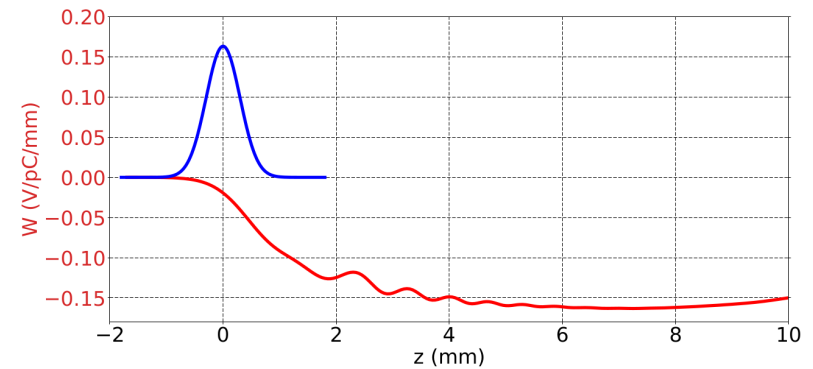


Figure : Transverse wakepotential in V/pC/mm of the ILC C-BPM, calculated with GdfidL for a vertical offset of 1 mm, Gaussian bunch length of 0.3 mm and 1 pC charge (in red). For reference, the distribution of the electrons in one bunch is shown (in blue).

Table: Positions of ILC BDS C-BPMs.

| BPM # | s (m) | BPM # | s (m) | BPM # | s (m) | BPM # | s (m) |
|-------|-------|-------|--------|-------|--------|-------|--------|
| 1 | 0.5 | 27 | 671.2 | 53 | 1247.1 | 79 | 1731.2 |
| 2 | 16.0 | 28 | 674.4 | 54 | 1261.1 | 80 | 1731.7 |
| 3 | 31.5 | 29 | 704.3 | 55 | 1265.1 | 81 | 1733.0 |
| 4 | 47.0 | 30 | 760.4 | 56 | 1279.1 | 82 | 1778.8 |
| 5 | 58.1 | 31 | 766.7 | 57 | 1429.0 | 83 | 1805.7 |
| 6 | 69.1 | 32 | 769.8 | 58 | 1468.2 | 84 | 1832.6 |
| 7 | 80.0 | 33 | 773.0 | 59 | 1481.0 | 85 | 1878.4 |
| 8 | 91.1 | 34 | 779.3 | 60 | 1495.0 | 86 | 1880.2 |
| 9 | 106.6 | 35 | 835.4 | 61 | 1509.0 | 87 | 1880.7 |
| 10 | 122.1 | 36 | 865.3 | 62 | 1510.7 | 88 | 1882.0 |
| 11 | 137.6 | 37 | 868.5 | 63 | 1537.9 | 89 | 1892.2 |
| 12 | 157.3 | 38 | 871.6 | 64 | 1565.1 | 90 | 1894.1 |
| 13 | 160.6 | 39 | 901.5 | 65 | 1566.7 | 91 | 1895.9 |
| 14 | 172.8 | 40 | 957.6 | 66 | 1580.7 | 92 | 1896.4 |
| 15 | 190.0 | 41 | 963.9 | 67 | 1594.7 | 93 | 1897.7 |
| 16 | 191.0 | 42 | 967.1 | 68 | 1607.9 | 94 | 2034.8 |
| 17 | 207.2 | 43 | 970.2 | 69 | 1614.9 | 95 | 2061.7 |
| 18 | 224.4 | 44 | 976.5 | 70 | 1654.4 | 96 | 2088.6 |
| 19 | 225.4 | 45 | 1013.8 | 71 | 1659.4 | 97 | 2242.8 |
| 20 | 241.6 | 46 | 1054.0 | 72 | 1697.6 | 98 | 2243.3 |
| 21 | 258.8 | 47 | 1058.0 | 73 | 1713.7 | 99 | 2243.4 |
| 22 | 259.8 | 48 | 1097.2 | 74 | 1715.5 | 100 | 2244.7 |
| 23 | 323.0 | 49 | 1135.4 | 75 | 1717.3 | 101 | 2247.4 |
| 24 | 326.5 | 50 | 1160.0 | 76 | 1719.2 | 102 | 2247.7 |
| 25 | 367.2 | 51 | 1184.6 | 77 | 1719.2 | 103 | 2247.7 |
| 26 | 466.5 | 52 | 1209.2 | 78 | 1729.4 | 104 | 2248.9 |

Impact of corrections in the ILC 250 and 500 GeV BDS

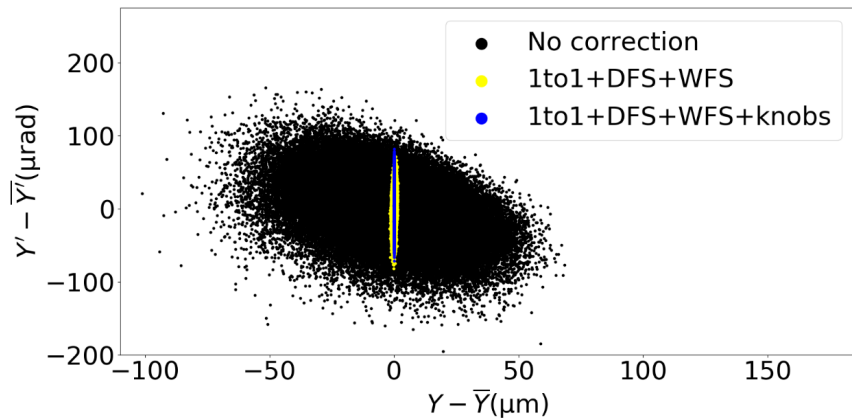


Figure : Centered vertical phase space at the 500 GeV ILC BDS IP, $Y' - \bar{Y}'$ vs. $Y - \bar{Y}$, for 3 cases: no correction, One-to-one steering, DFS, WFS and One-to-one steering, DFS, WFS and knobs, calculated with PLACET with wakefields.

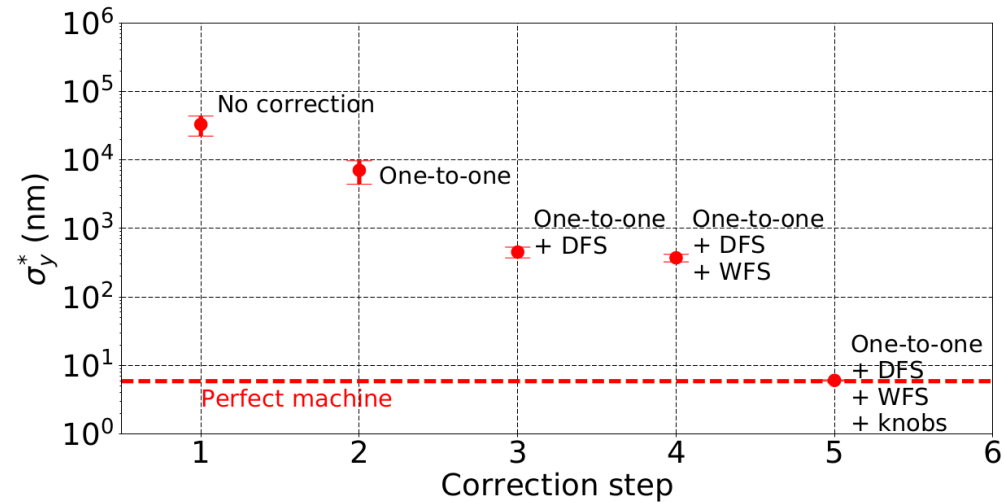


Table : Impact of the corrections on the ILC 250 GeV vertical beam size at the IP (σ_y^*) for 100 machines with wakefields and $2 \times 10^{10} e^-$, simulated with PLACET.

| Correction | $\bar{\sigma}_y^*$ |
|--------------------------------|-----------------------------|
| No correction | $69.4 \pm 26.8 \mu\text{m}$ |
| One-to-one | $1.1 \pm 0.3 \mu\text{m}$ |
| One-to-one + DFS | $514 \pm 65 \text{ nm}$ |
| One-to-one + DFS + WFS | $512 \pm 64 \text{ nm}$ |
| One-to-one + DFS + WFS + knobs | $9.43 \pm 0.30 \text{ nm}$ |

Table : Impact of the corrections on the 500 GeV ILC vertical beam size at the IP (σ_y^*) for 100 machines with wakefields and $2 \times 10^{10} e^-$, simulated with PLACET.

| Correction | $\bar{\sigma}_y^*$ |
|--------------------------------|-----------------------------|
| No correction | $33.0 \pm 10.7 \mu\text{m}$ |
| One-to-one | $7.1 \pm 2.6 \mu\text{m}$ |
| One-to-one + DFS | $452 \pm 81 \text{ nm}$ |
| One-to-one + DFS + WFS | $372 \pm 47 \text{ nm}$ |
| One-to-one + DFS + WFS + knobs | $6.11 \pm 0.30 \text{ nm}$ |

Impact of short-range wakefields in the 250 and 500 GeV BDS

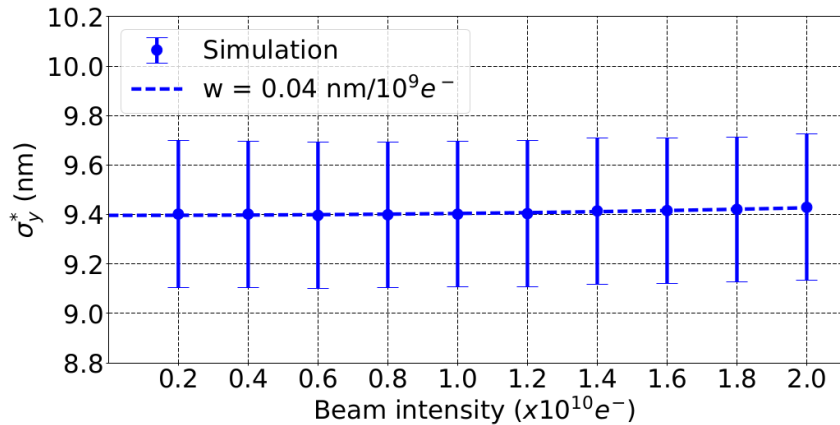


Figure 1: Vertical IP beam size σ_y^* vs. beam intensity in the 250 GeV BDS, calculated with PLACET with wakefields.

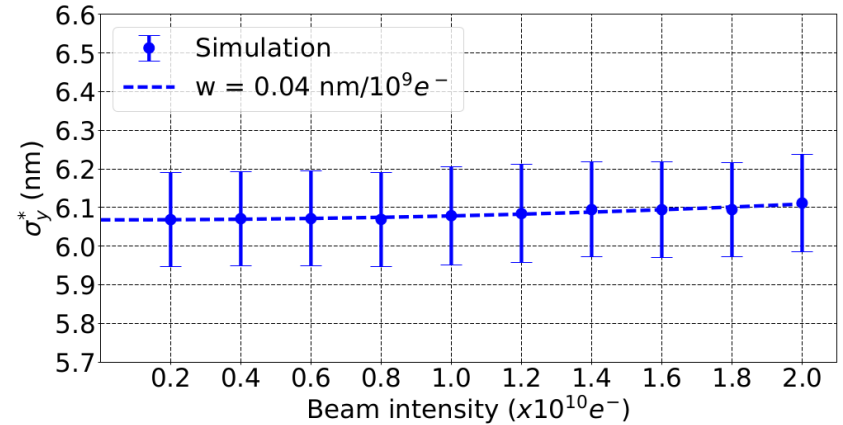


Figure 2: Vertical IP beam size σ_y^* vs. beam intensity in the 500 GeV BDS, calculated with PLACET with wakefields.

Table 1: Intensity-dependent effects due to wakefields on the vertical IP beam size σ_y^* in the 250 GeV ILC BDS, calculated with PLACET with wakefields.

| Beam intensity | $\overline{\sigma_y^*}$ (nm) | w (nm/ $10^9 e^-$) |
|--------------------------|------------------------------|---------------------|
| $0.2 \times 10^{10} e^-$ | 9.40 ± 0.30 | 0.04 |
| $2.0 \times 10^{10} e^-$ | 9.43 ± 0.30 | |

Table 2: Intensity-dependent effects due to wakefields on the vertical IP beam size σ_y^* in the 500 GeV BDS, calculated with PLACET with wakefields.

| Beam intensity | $\overline{\sigma_y^*}$ (nm) | w (nm/ $10^9 e^-$) |
|--------------------------|------------------------------|---------------------|
| $0.2 \times 10^{10} e^-$ | 6.07 ± 0.30 | 0.04 |
| $2.0 \times 10^{10} e^-$ | 6.11 ± 0.30 | |

Short-range wakefield effects are negligible in both 250 and 500 GeV BDS

$$w [nm/10^9 e^-] = \frac{(\sqrt{\sigma_{y,q}^2 - \sigma_{y,0}^2})}{q}$$

Simulations of the impact of long-range wakefields

In the 250 GeV ILC BDS

Long-range wakefields in the ILC BDS

Resistive walls wakefield

- Electrons going through the pipe interacts with the surrounding structure and generates a wake field.
- This wake field produces a transverse kick for the following bunches.
- The following model is used for the transverse wake function [9]:

$$W(z) = \frac{c}{\pi b^3} \sqrt{\left(\frac{Z_0}{\sigma_r \pi z}\right)} L$$

With b the radius of the beam pipe, Z_0 the impedance of the vacuum, σ_r the conductivity of the pipe and L the length of the beam line element.

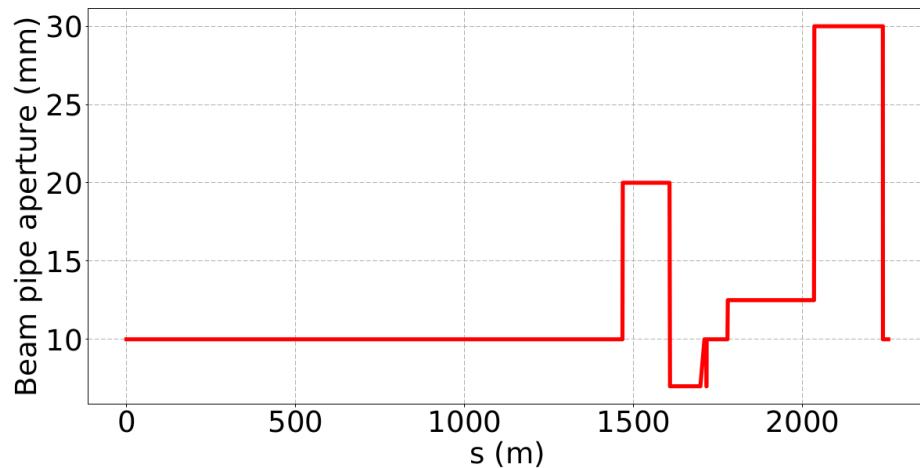
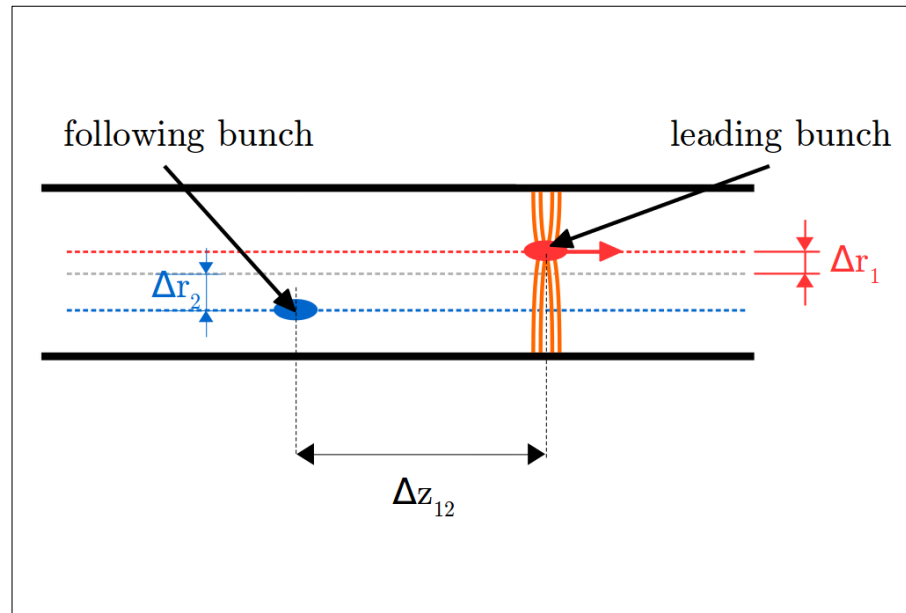


Figure: The ILC BDS beam aperture profile vs. s .

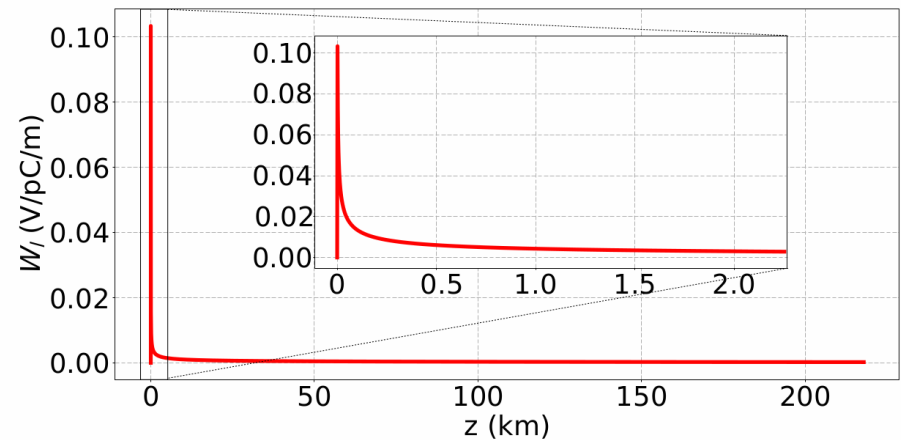
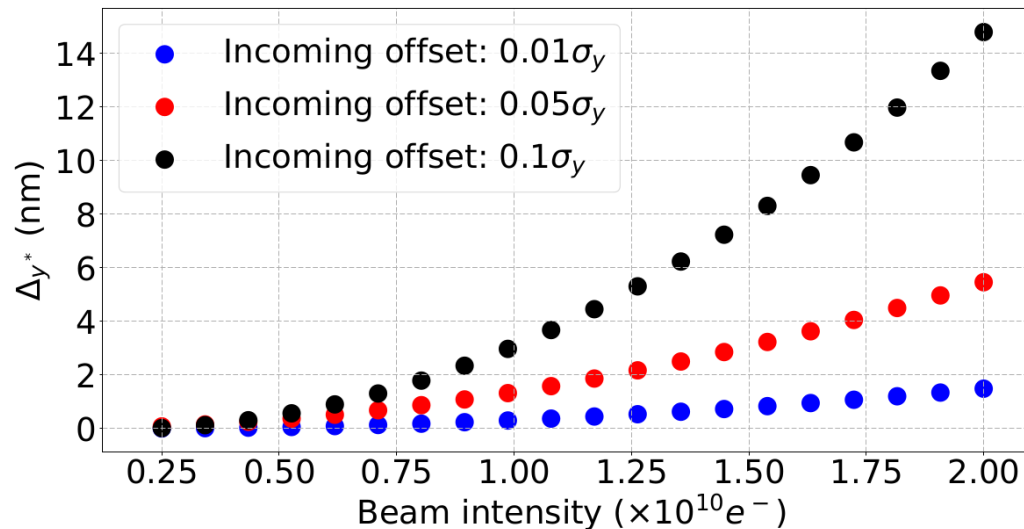


Figure : The ILC resistive walls wakepotential for a copper beam pipe with a constant radius of 10 mm for the length of a train (~218 km). The zoom shows the wakepotential for the length of the ILC BDS (~2254 m).

Impact of long-range wakefields in the 250 GeV ILC BDS for a constant offset

Simulation procedure:

- A train of 1312 bunches is injected at the entrance of the BDS.
- Each bunch is made of one macro-particle.
- Incoming position and angle offset of the train to study the impact of long-range wakefields. Amplitude of the incoming offsets: 0.01 , 0.05 , $0.1\sigma_y$ or σ_y , with σ_y and $\sigma_{y'}$ the beam size and the beam divergence at the entrance of the BDS.



$$\sigma_y = 0.82 \mu m$$

$$\sigma_{y'} = 0.097 \mu rad$$

Figure : Vertical orbit deflection at the IP between the first and last bunch of a train Δy^* vs. beam intensity for three incoming constant position offsets of the train of bunches in the 250 GeV ILC BDS: $0.01\sigma_y$, $0.05\sigma_y$ and $0.1\sigma_y$, calculated with PLACET with resistive wall effects included.

Impact of long-range wakefields in the 250 GeV ILC BDS for a constant offset

- Study of the impact of long-range wakefields for a train injected in the BDS with a constant vertical position and an angle offset of $0.01\sigma_y$ and $0.01\sigma_{y'}$, respectively on the vertical orbit deflection at the IP normalized by the IP beam size, $\Delta y^*/\sigma_y^*$ (left).
- Same study was done for both vertical and horizontal incoming offsets (right).

$$\sigma_{y'} = 0.097 \mu\text{rad} \quad \sigma_y = 0.82 \mu\text{m} \quad \sigma_y^* = 7.7 \text{ nm}$$

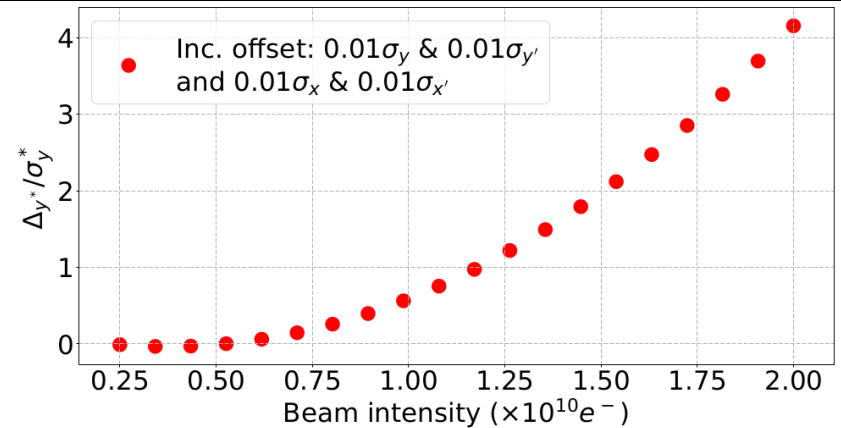
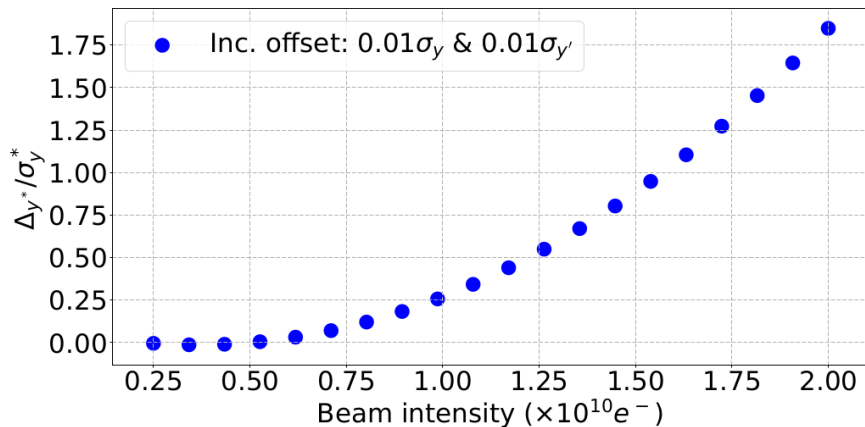


Figure 1: Vertical orbit deflection at the IP between the first and last bunch of a train normalised by the IP vertical beam size ($\Delta y^*/\sigma_y^*$) vs. beam intensity for a train with incoming constant position and angle offsets of respectively $0.01\sigma_y$ and $0.01\sigma_{y'}$ in the 250 GeV ILC BDS, calculated with PLACET with resistive wall effects included.

Figure 2: Vertical orbit deflection at the IP between the first and last bunch of a train normalised by the IP vertical beam size ($\Delta y^*/\sigma_y^*$) vs. beam intensity for a train with incoming constant horizontal position and angle offsets of respectively $0.01\sigma_x$ and $0.01\sigma_{x'}$ and vertical incoming position and angle offsets of respectively $0.01\sigma_y$ and $0.01\sigma_{y'}$ in the 250 GeV ILC BDS, calculated with PLACET with resistive wall effects included.

Impact of long-range wakefields in the 250 GeV ILC BDS for a random offset

- Study of the impact of long-range wakefields for a train injected in the BDS with a random horizontal and vertical position and an angle offsets.
- The distribution of random incoming position and angle offset is a normal distribution with a zero mean and variance of 2.6×10^{-4} , leading to a $\pm 5\%$ incoming vertical and horizontal angle and position offsets.

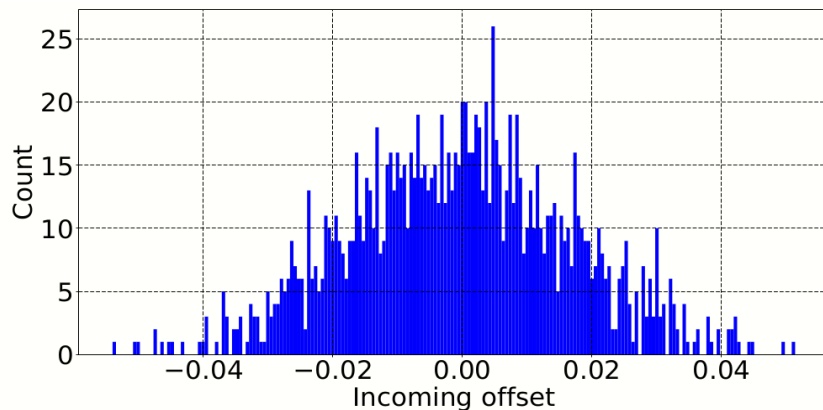


Figure : Distribution of incoming position and angle offsets from $-0.05\sigma_{x,y}$ to $0.05\sigma_{x,y}$.

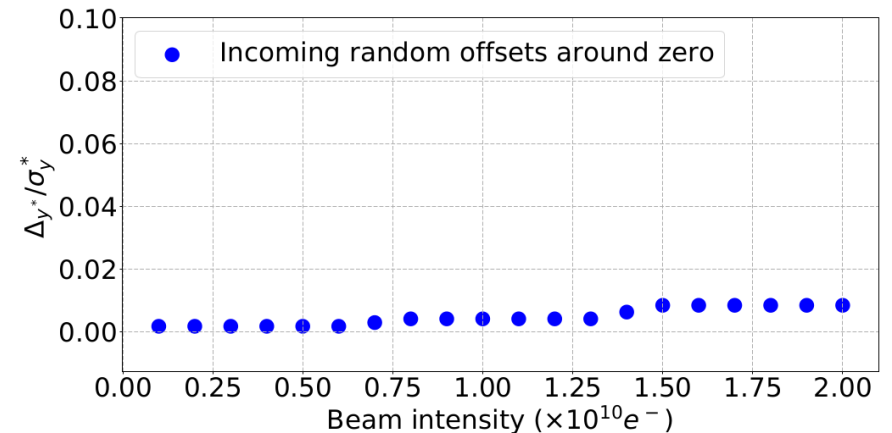


Figure : Vertical orbit deflection at the IP between the first and last bunch of a train normalised by the IP vertical beam size ($\Delta y^*/\sigma_y^*$) vs. beam intensity for a train with a random and around zero incoming vertical and horizontal position and angle offsets of between -0.05 and 0.05σ in the 250 GeV ILC BDS, calculated with PLACET with resistive wall effects included.

Random incoming offsets lead to a negligible effect of long-range wakefields

Impact of long-range wakefields in the 250 GeV ILC BDS Luminosity

- Study of the impact of luminosity degradation due to the vertical orbit deflection at the IP with Guinea-Pig, a code simulating the impact of beam-beam effects on luminosity and background [10].

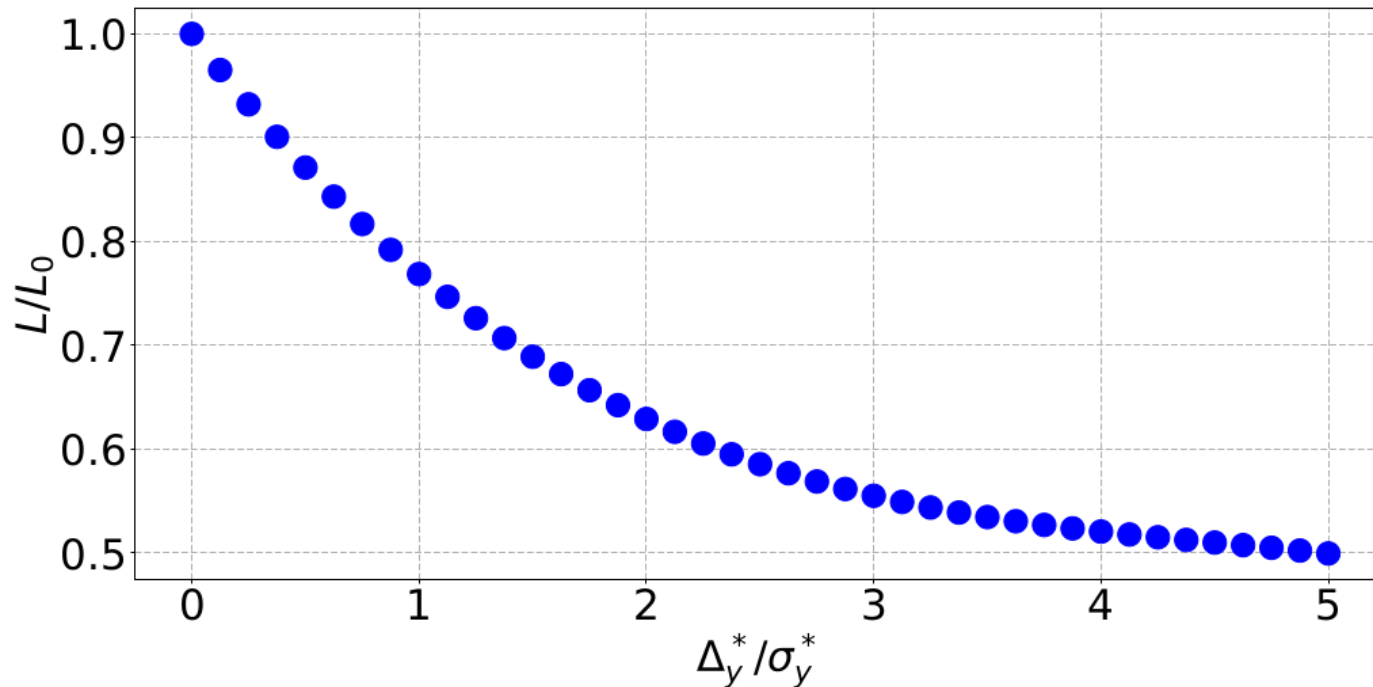


Figure : 250 GeV ILC luminosity degradation vs. relative vertical offset of the colliding beams.

$$L = f_{coll} \frac{n_1 n_2}{4\pi \sigma_x^* \sigma_y^*} F$$

Impact of long-range wakefields in the 250 GeV ILC BDS Summary

Table : Impact of different incoming vertical position and angle offsets on the relative vertical offset at the IP (Δ_y^*) and the luminosity for low and high beam intensities in the 250 GeV ILC BDS.

| Case | Δ_y^* [nm] | Δ_y^*/σ_y^* | L/L_0 |
|-------------------------------------------------------------------------------------------------------------------------------------------------------|-------------------|-------------------------|------------|
| Inc. position offset $0.1\sigma_y$ | | | |
| $0.2 \times 10^{10} e^-$ | 0.013 | 0.002 | ~ 1.0 |
| $2.0 \times 10^{10} e^-$ | 14.8 | 1.92 | 0.64 |
| Inc. angle offset $0.1\sigma_{y'}$ | | | |
| $0.2 \times 10^{10} e^-$ | 0.015 | 0.002 | ~ 1.0 |
| $2.0 \times 10^{10} e^-$ | 127 | 16.5 | 0.25 |
| Inc. offsets $0.01\sigma_y$ & $0.01\sigma_{y'}$ | | | |
| $0.2 \times 10^{10} e^-$ | 0.039 | 0.005 | ~ 1.0 |
| $2.0 \times 10^{10} e^-$ | 14.2 | 1.85 | 0.53 |
| Inc. offsets $0.01\sigma_y$ & $0.01\sigma_{y'}$ and $0.01\sigma_x$ & $0.01\sigma_{x'}$ | | | |
| $0.2 \times 10^{10} e^-$ | 2.77 | 0.36 | 0.87 |
| $2.0 \times 10^{10} e^-$ | 32.0 | 4.15 | 0.36 |
| Inc. random offsets around zero | | | |
| $0.2 \times 10^{10} e^-$ | 0.100 | 0.013 | ~ 1.0 |
| $2.0 \times 10^{10} e^-$ | 0.501 | 0.065 | 0.98 |

Long-range wakefields have a significant impact in the 250 GeV ILC BDS. An intra-train feedback system would be necessary in order to achieve the luminosity goals.

Impact of long-range wakefields in the 500 GeV ILC BDS

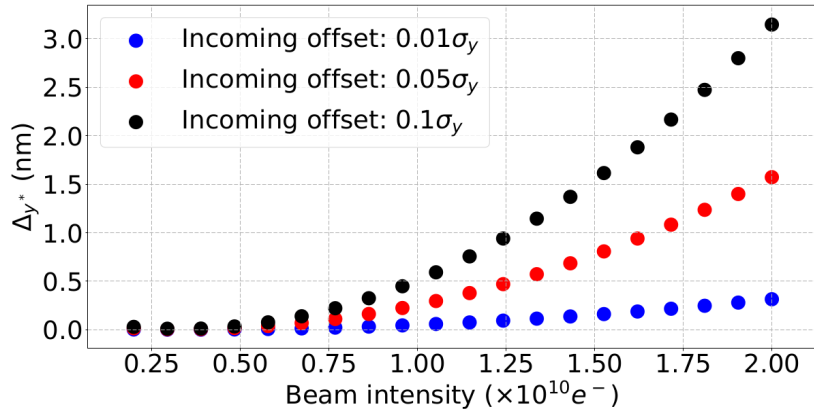


Figure 1: Vertical orbit deflection at the IP between the first and last bunch of a train Δy^* vs. beam intensity for three incoming constant position offsets of the train of bunches in the 500 GeV ILC BDS: $0.01\sigma_y$, $0.05\sigma_y$ and $0.1\sigma_y$, calculated with PLACET with resistive wall effects included.

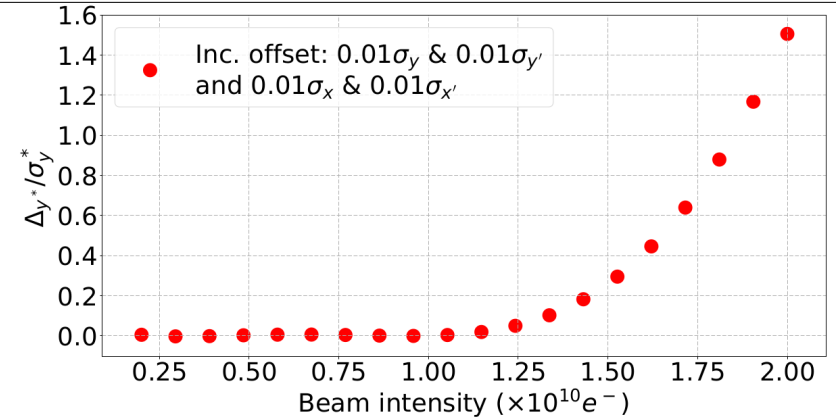


Figure 2: Vertical orbit deflection at the IP between the first and last bunch of a train normalised by the IP vertical beam size ($\Delta y^*/\sigma_y^*$) vs. beam intensity for a train with incoming constant horizontal position and angle offsets of respectively $0.01\sigma_x$ and $0.01\sigma_{x'}$ and vertical incoming position and angle offsets of respectively $0.01\sigma_y$ and $0.01\sigma_{y'}$ in the 500 GeV ILC BDS, calculated with PLACET with resistive wall effects included.

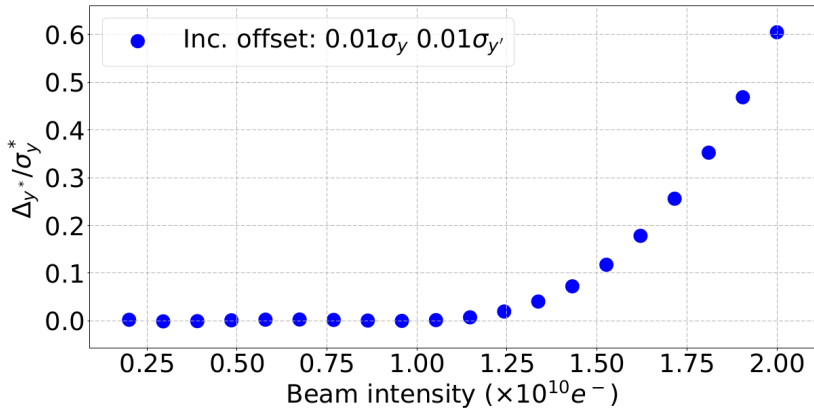


Figure 3: Vertical orbit deflection at the IP between the first and last bunch of a train normalised by the IP vertical beam size ($\Delta y^*/\sigma_y^*$) vs. beam intensity for a train with incoming constant position and angle offsets of respectively $0.01\sigma_y$ and $0.01\sigma_{y'}$ in the 500 GeV ILC BDS, calculated with PLACET with resistive wall effects included.

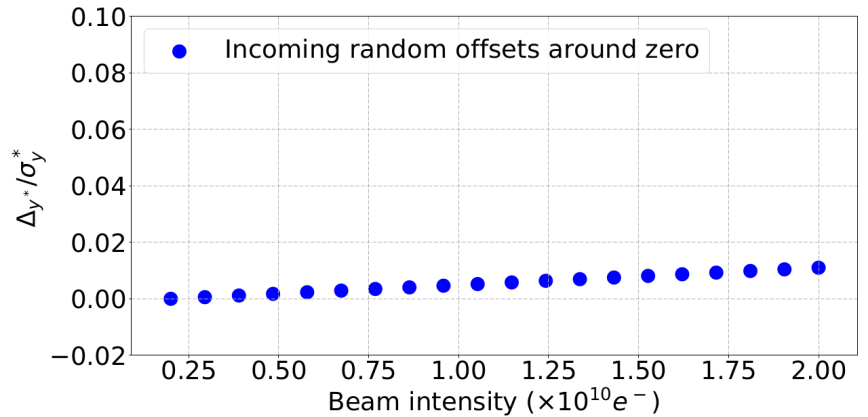


Figure 4: Vertical orbit deflection at the IP between the first and last bunch of a train normalised by the IP vertical beam size ($\Delta y^*/\sigma_y^*$) vs. beam intensity for a train with a random and around zero incoming vertical and horizontal position and angle offsets of between -0.05 and 0.05σ in the 500 GeV ILC BDS, calculated with PLACET with resistive wall effects included.

Impact of long-range wakefields in the 500 GeV ILC BDS Luminosity

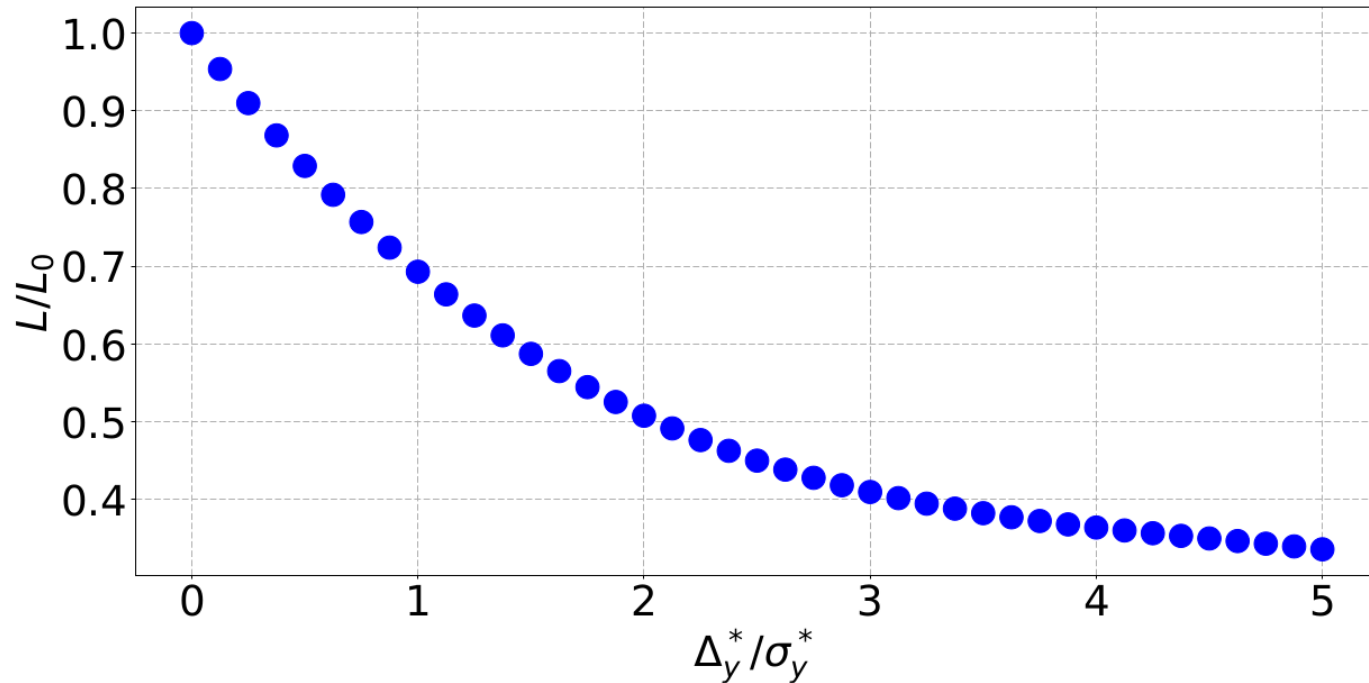


Figure : 500 GeV ILC BDS luminosity degradation vs. relative vertical offset of the colliding beams.

$$L = f_{coll} \frac{n_1 n_2}{4\pi \sigma_x^* \sigma_y^*} F$$

Impact of long-range wakefields in the 500 GeV ILC BDS Summary

Table : Impact of different incoming vertical position and angle offsets on the relative vertical offset Δ_y^* at the IP and the luminosity for low and high beam intensities in the ILC BDS 500 GeV.

| Case | Δ_y^* [nm] | Δ_y^*/σ_y^* | L/L_0 |
|-------------------------------------------------------------------------------------------------------------------------------------------------------|-------------------|-------------------------|------------|
| Inc. position offset $0.1\sigma_y$ | | | |
| $0.2 \times 10^{10} e^-$ | 0.028 | 0.005 | ~ 1.0 |
| $2.0 \times 10^{10} e^-$ | 3.08 | 0.522 | 0.82 |
| Inc. angle offset $0.1\sigma_{y'}$ | | | |
| $0.2 \times 10^{10} e^-$ | 0.0178 | 0.003 | ~ 1.0 |
| $2.0 \times 10^{10} e^-$ | 32.57 | 5.52 | 0.32 |
| Inc. offsets $0.01\sigma_y$ & $0.01\sigma_{y'}$ | | | |
| $0.2 \times 10^{10} e^-$ | 0.012 | 0.002 | ~ 1.0 |
| $2.0 \times 10^{10} e^-$ | 3.54 | 0.6 | 0.80 |
| Inc. offsets $0.01\sigma_y$ & $0.01\sigma_{y'}$ and $0.01\sigma_x$ & $0.01\sigma_{x'}$ | | | |
| $0.2 \times 10^{10} e^-$ | 0.03 | 0.005 | ~ 1.0 |
| $2.0 \times 10^{10} e^-$ | 8.91 | 1.51 | 0.59 |
| Inc. random offsets around zero | | | |
| $0.2 \times 10^{10} e^-$ | 0.01 | 0.002 | ~ 1.0 |
| $2.0 \times 10^{10} e^-$ | 0.06 | 0.01 | ~ 1.0 |

Long-range wakefields have a significant impact in the 500 GeV ILC BDS as well. An intra-train feedback system would be necessary in order to achieve the luminosity goals.

Conclusion and outlook

- The intensity-dependent effects due to short-range wakefields are negligible in both the 250 and 500 GeV ILC BDS. The intensity-dependent parameter w is around 0.04 nm/10⁹ e for both energies, representing an increase on the vertical beam size at the IP of 0.03 nm and 0.04 nm for 250 GeV and 500 GeV respectively.
- The intensity-dependent effects due to long-range wakefields have a significant impact on the luminosity. Indeed, at 2.0×10^{10} e⁻, the impact of incoming vertical and horizontal position offsets of $0.01\sigma_y$ and $0.01\sigma_x$ respectively, and incoming vertical and horizontal angle offsets of $0.01\sigma_y'$ and $0.01\sigma_x'$ respectively leads to a luminosity loss of 64% in the 250 GeV BDS and of 41% in the 500 GeV BDS.
- An intra-train feedback system is necessary in order to correct those effects and to achieve the required luminosity goals. Such a system has been studied to correct the vertical jitters generated by ground motion [11].
- A prototype feedback system was tested in ATF2 and gave promising results [12]. The next step will be to implement this feedback and study its impact on the luminosity losses due to intensity-dependent effects.

Thank you